

Neutrino masses twenty–five years later

J. W. F. Valle

*Instituto de Física Corpuscular, C.S.I.C. – Universitat de València
Edificio de Institutos de Paterna, Apartado 22085, E-46071 València, Spain*

and

*Institut für Theoretische Physik, Auf der Morgenstelle 14
Universität Tübingen, D-72076 Tübingen, Germany*

Abstract.

The discovery of neutrino mass marks a turning point in elementary particle physics, with important implications for nuclear and astroparticle physics. Here I give a brief update, where I summarize the current status of three–neutrino oscillation parameters from current solar, atmospheric, reactor and accelerator neutrino data, discuss the case for sterile neutrinos and LSND, and also the importance of tritium and double beta decay experiments probing the absolute scale of neutrino mass. In this opinionated look at the present of neutrino physics, I keep an eye in the future, and a perspective of the past, taking the opportunity to highlight Joe Schechter’s pioneering contribution, which I have had the fortune to share, as his PhD student back in the early eighties.

INTRODUCTION

The basic theoretical setting required for the description of current neutrino oscillation experiments [1, 2, 3, 4, 5] was laid out in the early eighties [6, 7, 8, 9]. This included the two-component quantum description of massive Majorana neutrinos and the gauge theoretic characterization of the lepton mixing matrix describing neutrino oscillations [6]. To complete the formulation of neutrino oscillations necessary to describe current data the other important ingredient was the formulation of the theory of neutrino oscillations in matter by Mikheev, Smirnov and Wolfenstein [10, 11]¹. The theoretical origin of neutrino mass remains as much of a mystery today as it was back in the eighties. Much of the early effort devoted to the study of neutrino masses was motivated in part by the idea of unification which introduced the seesaw mechanism [15, 16], and by the (later unconfirmed) hints for neutrino oscillations then seen by Reines [17]. The basic

¹ For recent reviews see [12, 13, 14] and references therein.

dimension–five neutrino mass operator [18] arises in the context of the $SO(10)$ unification group, though it was soon realized that the seesaw idea can be applied to left-right symmetric theories [9], or the simplest effective Standard Model gauge framework [6]. While the $SO(10)$ or $SU(2)_L \otimes SU(2)_R \otimes U(1)$ formulations of the seesaw have the virtue of relating the small neutrino mass to the dynamics of parity (gauged B-L) violation, the effective $SU(2) \otimes U(1)$ description is more general and applies to any theory, for example with ungauged B-L [19, 20]. The role of a Higgs triplet in generating neutrino masses was noted in the early days, either on its own or as part of the seesaw mechanism [6, 7, 9]². The detailed general structure of the seesaw diagonalizing matrix given in Ref. [20] plays a role in the determination of the baryon asymmetry of the Universe, within the so-called leptogenesis scenarios [21, 22].

A radical approach to the seesaw idea is that of neutrino unification, recently advocated in [23] and [24] leads naturally to a quasi degenerate neutrino spectrum with important phenomenological implications.

However, it is worth stressing that the seesaw is only one way of generating the basic dimension–five neutrino mass operator [18], which may arise from physics “just around the corner”, such as low energy supersymmetry [25, 26, 27]. For example, schemes with spontaneously broken R parity [28, 29, 30] lead effectively to bilinear R parity violation [31]. Neutrino mixing angles can be tested at accelerator experiments [32, 33, 34]. Other variants of this idea involve triplet Higgs bosons, such as the model in [35]. Alternative low energy mechanisms for neutrino mass generation are the models of Babu [36] and Zee [37] and variants thereof.

Much is now known about the structure of the lepton mixing matrix since the paper in Ref. [6] has been written. First, LEP data imply three light sequential $SU(2) \otimes U(1)$ doublet (active) neutrinos [38], ν_e , ν_μ and ν_τ . This still leaves open the possibility of singlet leptons remaining as light as the electron-volt range, due to some symmetry [39, 40, 41]. In this case they might take part in the oscillations as sterile neutrinos [42], as hinted by the data of LSND [43]. While this experiment is currently unconfirmed, a global analysis of all current oscillation experiments strongly prefer the minimal three light–neutrino hypothesis [44, 45]. The possibility of symmetric (2+2) schemes is ruled out, because in this case sterile neutrinos take part in both solar and atmospheric oscillations. On the other hand the presence of a light sterile neutrino in a (3+1) scheme is still allowed, since

² Such triplet contribution to neutrino mass may come from an induced vacuum expectation value.

it can be chosen to decouple from solar and atmospheric oscillations, though strongly disfavoured by short-baseline experiments.

Data from cosmology, including CMB data from WMAP [46] [47, 48, 49] and the 2dFGRS large scale structure surveys [50] lead to further restrictions, especially on large Δm_{LSND}^2 values³. The three–neutrino lepton mixing matrix is characterized by three mixing angles: θ_{12} which describes solar neutrino oscillations, θ_{23} which characterizes atmospheric neutrino oscillations, and θ_{13} which couples these two analyses. It can be written as

$$K = \omega_{12}\omega_{13}\omega_{23}$$

where ω_{ij} is a complex rotation in the ij sector. This parametrization can be found in [6]. The charged current lepton mixing matrix also contains one Kobayashi–Maskawa–like leptonic CP phase whose effects are suppressed due to the stringent limits on θ_{13} following mainly from reactor data [51]. Moreover they are suppressed by the small mass splitting indicated by the solar neutrino data analysis (see below). This happens since, in the 3-neutrino limit, CP violation disappears as two neutrinos become degenerate [52]. The effect of this phase in current neutrino oscillation experiments is negligible. Future neutrino factories [53, 54, 55, 56] aim to be sensitive to such CP violating effects. There are, in addition, two CP phases associated with the (12) and (23) sectors, that can not be removed by field redefinition due to the Majorana nature of neutrinos [6]. However these non–Kobayashi–Maskawa–like CP phases drop out from conventional oscillation experiments. All CP phases are neglected in current oscillation analyses, which take the matrices ω_{ij} as real rotations.

However these Majorana phases do affect lepton-number-violating oscillations [57]. Unfortunately, these are strongly suppressed by the small masses of neutrinos and the V-A nature of the weak interaction. Massive majorana neutrinos are also expected to have non-zero transition magnetic moments [8], sensitive to the Majorana phases [8, 58, 59]. However magnetic moments also vanish in the limit of massless neutrinos [60]. Neutrinoless double beta decay [61, 62] holds better chances of revealing the effects of these extra phases. However nuclear physics uncertainties currently preclude a realistic way to test them [63].

³ Note that it is not possible to rule out light sterile states if they do not mix significantly with the three sequential active neutrinos. Though heavy isosinglet leptons would not be emitted in weak decays, they would lead to an effectively non-unitary lepton mixing matrix characterizing the three active neutrinos [6].

NEUTRINO DATA ANALYSIS

Neutrino masses have been discovered in atmospheric neutrinos [1]. In contrast solar neutrino experiments could not establish neutrino oscillations [64, 65] without the results of KamLAND. An analysis of recent solar, atmospheric and reactor data ⁴ has been given in [44] ⁵. This paper presents a generalized determination of the neutrino oscillation parameters taking into account that both the solar ν_e and the atmospheric ν_μ may convert to a mixture of active and sterile neutrinos. This allows one to systematically combine solar and atmospheric data with the current short baseline neutrino oscillation data including the LSND evidence for oscillations [45].

Insofar as atmospheric data are concerned, the analysis in [44] used the data given in Refs. [66, 67, 68, 69] as well as the most recent atmospheric Super-K (1489-day) [70] and MACRO [71] data.

The solar neutrino data include rates for the Homestake chlorine experiment [72] ($2.56 \pm 0.16 \pm 0.16$ SNU), the most recent result of the gallium experiments SAGE [73] ($70.8^{+5.3}_{-5.2} \text{ }^{+3.7}_{-3.2}$ SNU) and GALLEX/GNO [74] ($70.8 \pm 4.5 \pm 3.8$ SNU), as well as the 1496-days Super-K data sample [2]. The latter are presented in the form of 44 bins (8 energy bins, 6 of which are further divided into 7 zenith angle bins). In addition, we have the latest SNO results in Refs. [3], in the form of 34 data bins (17 energy bins for each day and night period). All in all, $3 + 44 + 34 = 81$ observables.

Moreover, in version 3 of the arXiv the implications of the first 145.1 days of KamLAND data on the determination of the solar neutrino parameters are also discussed in detail, updating the published version [44].

Atmospheric + reactor

The atmospheric plus reactor data can be well described in the approximation $\Delta m_{\text{SOL}}^2 \ll \Delta m_{\text{ATM}}^2$, taking the electron neutrino as completely decoupled from atmospheric oscillations, with $\theta_{13} \rightarrow 0$ (for the case $\theta_{13} \neq 0$ see below).

The observed zenith angle distributions of atmospheric neutrino events and those expected in the Standard Model and within various oscillation hypothesis are given in

⁴ See Ref. [44] for an extensive list of solar and atmospheric neutrino experiments.

⁵ For a discussion of other neutrino oscillation analyses see Table 1 in [12] and Table 2 in [44]

Fig. 1. Clearly, active neutrino oscillations describe the data very well indeed. In con-

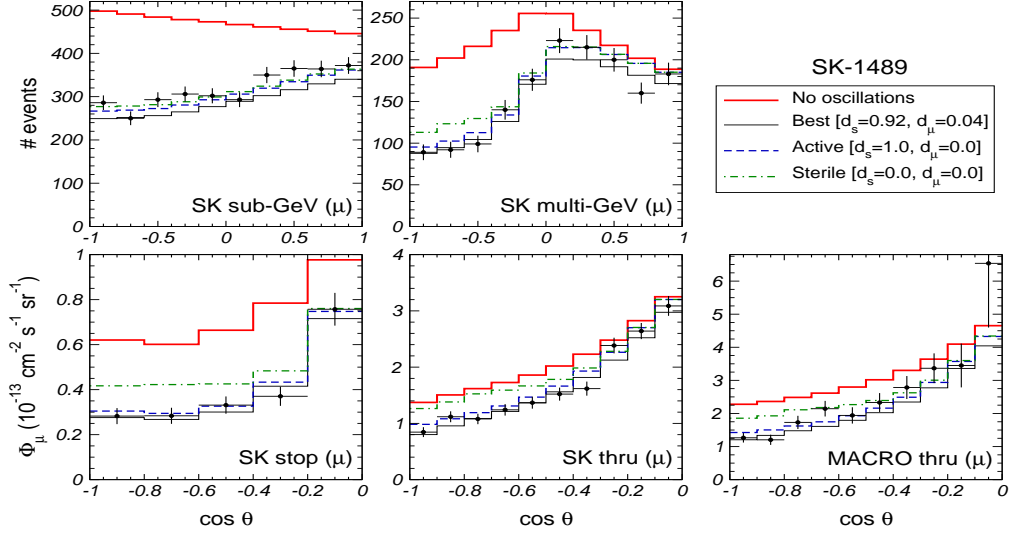


FIGURE 1. Zenith angle dependence of the μ -like atmospheric neutrino data from Ref. [44]. From the figure one can compare the predicted number of atmospheric neutrino events for best-fit, pure-active and pure-sterile oscillations and no oscillations.

trast, the no-oscillations hypothesis is clearly ruled out. On the other hand, conversions to sterile neutrinos lead to an excess of events for neutrinos crossing the core of the Earth, in all the data samples except sub-GeV.

The parameters θ_{ATM} and Δm_{ATM}^2 determined from the fit are summarized in Figs. 2 and 3. The latter considers several cases: arbitrary d_s and d_μ , best-fit d_s and d_μ , and

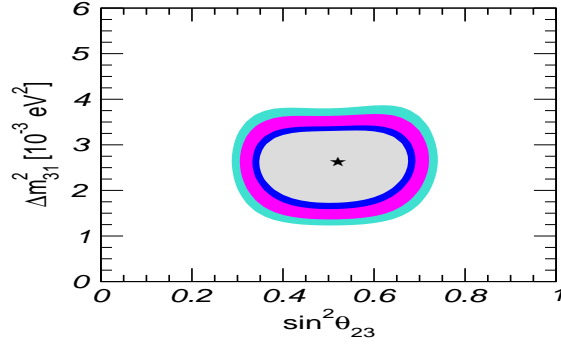


FIGURE 2. Allowed $\sin^2 \theta_{\text{ATM}}$ and Δm_{ATM}^2 values at 90%, 95%, 99% C.L. and 3σ corresponding to the latest atmospheric neutrino data, from [44].

pure active and mixed active-sterile neutrino oscillations. The meaning of these d -parameters, not taken into account by the Super-K collaboration, is discussed in [75]. Their existence is understood from the structure of the 4-neutrino lepton mixing matrix [6]. In conclusion, one finds that the improved fit of the atmospheric data lead to a more stringent constraint on the sterile component in atmospheric oscillations: if the

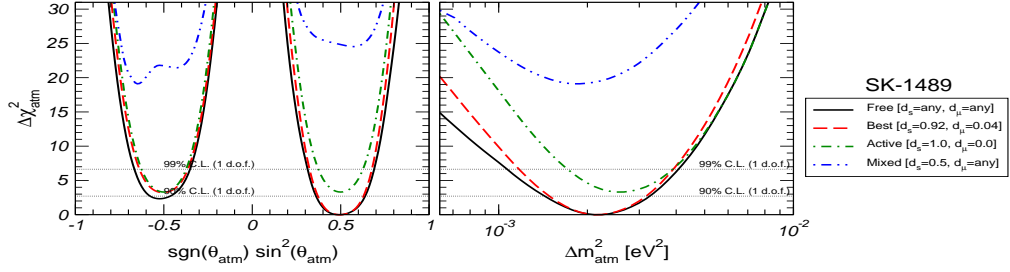


FIGURE 3. $\Delta\chi^2_{\text{ATM}}$ as a function of Δm^2_{ATM} , $\sin^2\theta_{\text{ATM}}$, d_s and d_μ , optimizing over the undisplayed parameters [44].

ν_μ is restricted to the atmospheric mass states only a sterile admixture of 16% is allowed at 99% C.L. while a bound of 35% is obtained in the unconstrained case. Pure sterile oscillations are disfavored with a $\Delta\chi^2 = 34.6$ compared to the pure active case.

Solar

In the presence of light sterile neutrinos the electron neutrino produced in the sun converts to ν_x (a combination of ν_μ and ν_τ) and a sterile neutrino ν_s : $\nu_e \rightarrow \sqrt{1-\eta_s}\nu_x + \sqrt{\eta_s}\nu_s$. The solar neutrino data are fit with three parameters: Δm^2_{SOL} , θ_{SOL} and the parameter $0 \leq \eta_s \leq 1$ describing the sterile neutrino fraction.

In Fig. 4 we display the regions of solar neutrino oscillation parameters for 3 d.o.f. with respect to the global minimum, for the standard case of active oscillations, $\eta_s = 0$. Notice that the SNO NC, spectral, and day-night data lead to an improved determination of the oscillation parameters: the shaded regions after their inclusion are much smaller than the hollow regions delimited by the corresponding $\text{SNO}_{\text{CC}}^{\text{rate}}$ confidence contours. This is especially important in closing the LMA-MSW region from above: values of $\Delta m^2_{\text{SOL}} > 10^{-3} \text{ eV}^2$ appear only at more than 3σ . Previous solar data on their own could not close the LMA-MSW region, only the inclusion of reactor data [51] probed the upper part of the LMA-MSW region [76]. The complete $\text{SNO}_{\text{CC,NC}}^{\text{SP,DN}}$ information is also important in excluding maximal solar mixing in the LMA-MSW region at 3σ .

Fig. 5 gives the profiles of $\Delta\chi^2_{\text{SOL}}$ as a function of Δm^2_{SOL} (left), $\tan^2\theta_{\text{SOL}}$ (middle) as well as η_s (right), by minimizing with respect to the undisplayed oscillation parameters. In the left and middle panels the solid, dashed and dot-dashed lines correspond to $\eta_s = 0$, $\eta_s = 1$ and $\eta_s = 0.5$, respectively.

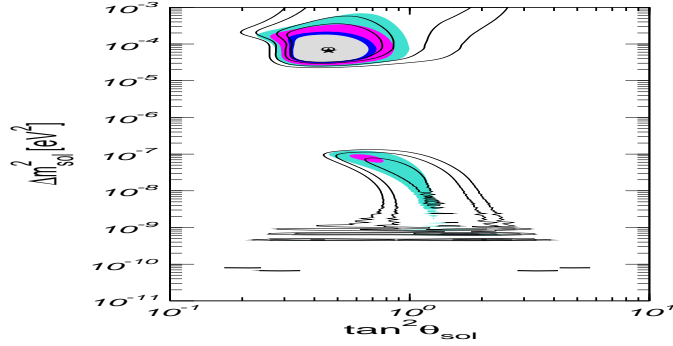


FIGURE 4. Allowed $\tan^2 \theta_{\text{SOL}}$ and Δm_{SOL}^2 regions for $\eta_s = 0$ (active oscillations). The lines and shaded regions correspond to the $\text{SNO}_{\text{CC}}^{\text{rate}}$ and $\text{SNO}_{\text{CC,NC}}^{\text{SP,DN}}$ analyses, respectively, as defined in Ref. [44]. The 90%, 95%, 99% C.L. and 3σ contours are for 3 d.o.f..

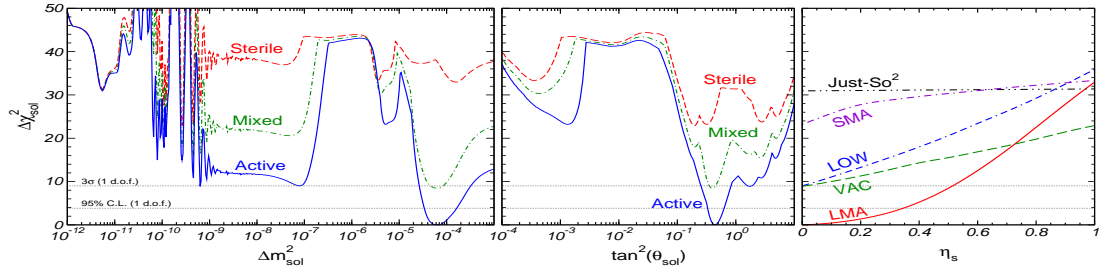


FIGURE 5. $\Delta\chi_{\text{SOL}}^2$ versus Δm_{SOL}^2 , $\tan^2 \theta_{\text{SOL}}$, and $0 \leq \eta_s \leq 1$ from global $\text{SNO}_{\text{CC,NC}}^{\text{SP,DN}}$ sample in Ref. [44].

Solar + KamLAND

The KamLAND collaboration has detected reactor neutrinos at the Kamiokande site coming from nuclear plants at distances 80-350 km away, with an average baseline of about 180 km, long enough to test the LMA-MSW region [5]. The target for the $\bar{\nu}_e$ flux is a spherical transparent balloon filled with 1000 tons of non-doped liquid scintillator, and the antineutrinos are detected via the inverse neutron β -decay process $\bar{\nu}_e + p \rightarrow e^+ + n$. KamLAND has for the first time observed the disappearance of neutrinos produced in a power reactor during their flight over such distances. The observed-to-expected event number ratio is $0.611 \pm 0.085(\text{stat}) \pm 0.041(\text{syst})$ for $\bar{\nu}_e$ energies > 3.4 MeV, giving the first terrestrial confirmation of the solar neutrino anomaly with man-produced neutrinos.

The impact of combining the first 145.1 days of KamLAND data with the full sample of solar neutrino data on the determination of neutrino oscillation parameters, is shown in Figs. 6 and 7, from [77]. One finds that non-oscillation solutions [64, 65] are now rejected at more than 3σ , while non-LMA-MSW oscillations are excluded at more than

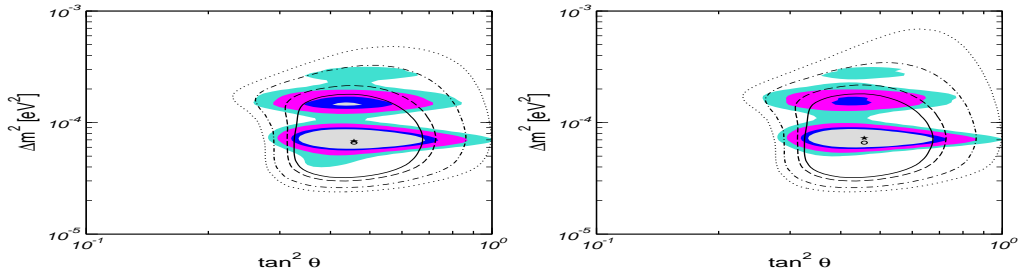


FIGURE 6. Allowed 90%, 95%, 99% and 99.73% C.L. regions (2 d.o.f.) from the global analysis of solar, Chooz and KamLAND data [77]. The hollow lines do not include KamLAND. Left is for Gaussian, right is for Poisson statistics. The star (dot) is the best fit point for combined (solar+Chooz only) analysis.

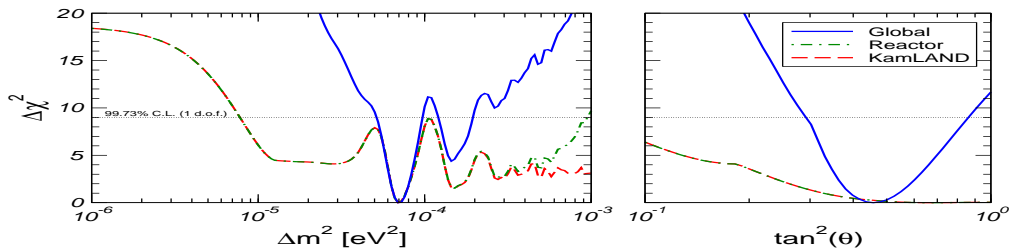


FIGURE 7. $\Delta\chi^2$ profiles versus Δm_{SOL}^2 and $\tan^2 \theta$ from [77]. The (red) dashed line refers to KamLAND alone. The (green) dot-dashed line corresponds to the full reactor data sample, including both KamLAND and Chooz. The (blue) solid line refers to the global analysis of the complete solar and reactor data.

4 σ . Furthermore, the new data have a strong impact in narrowing down the allowed range of Δm_{SOL}^2 inside the LMA-MSW region. In contrast, the new data have little impact on the location of the best fit point. In particular the solar neutrino mixing remains significantly non-maximal (3 σ).

The result for the fit shows a clear preference of the data for the pure active LMA-MSW solution of the solar neutrino problem, with the LOW, VAC, SMA-MSW and Just-So² solutions disfavored by a $\Delta\chi^2 = 22, 22, 36, 44$, respectively. The global solar data constrains the admixture of a sterile neutrino to be less than 43% at 99% C.L..

Robustness of the oscillation parameter determination

How robust is the determination of solar and atmospheric neutrino oscillation parameters, taking into account the possible existence of other non-standard neutrino properties? Many models of neutrino mass are accompanied by potentially sizable non-standard neutrino interactions, which may be flavour-changing (FC) or non-universal (NU), arising either from gauge [6] or Yukawa interactions [78]. These may affect neutrino prop-

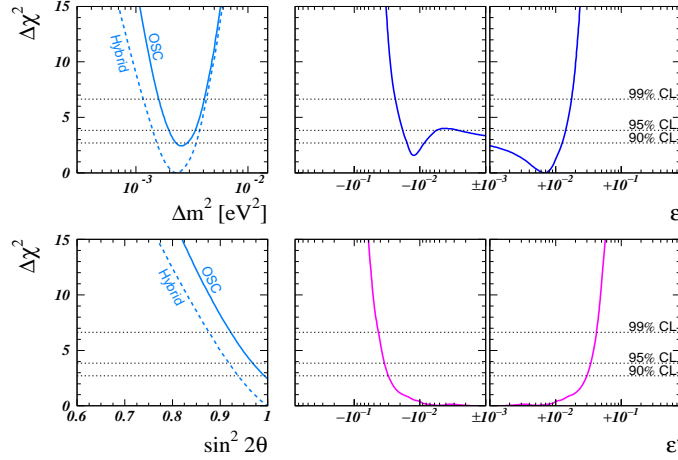


FIGURE 8. Behaviour of $\Delta\chi^2$ for the new Super-K and MACRO data, as a function of the oscillation parameters Δm^2 and θ (left panels), and of the NSI parameters ε and ε' (right panels) [82]. In the left panels both the pure oscillations case and the hybrid OSC + NSI mechanism are given. Optimizing over undisplayed parameters is performed in all cases.

agation properties in matter even in the massless limit [79, 80, 81].

In Ref. [82] the atmospheric neutrino anomaly has been reconsidered in light of the latest data from Super-K contained events and from Super-K and MACRO up-going muons. Neutrino evolution was described in terms of non-standard neutrino-matter interactions (NSI) and conventional ν_μ to ν_τ oscillations (OSC). The statistical analysis of the data shows that a pure NSI mechanism is now ruled out at 99%, while standard ν_μ to ν_τ oscillations provide an excellent description of the anomaly. Limits were derived on FC and NU neutrino interactions, as illustrated in Fig. 8. One sees that the off-diagonal flavour-changing neutrino parameter ε and the diagonal non-universality neutrino parameter ε' are confined to $-0.03 < \varepsilon < 0.02$ and $|\varepsilon'| < 0.05$ at 99.73% CL. These limits are model independent as they are obtained from pure neutrino-physics processes. The stability of the neutrino oscillation solution to the atmospheric neutrino anomaly against the presence of NSI establishes the robustness of the near-maximal atmospheric mixing and massive-neutrino hypothesis. The current sensitivity of atmospheric neutrino experiments to the existence of neutrino flavor changing NSI can be further improved with future neutrino factory experiments, especially for higher energies [83].

It has been shown that non-standard neutrino interactions give a very good interpretation of current solar neutrino data consistent with the oscillation description of the atmospheric neutrino data [65]. Such solutions, however, although preferred by the solar data, are ruled out by the first results of the KamLAND reactor experiment, at more

than 3σ [65]. Therefore NSI can not be the leading explanation of the solar neutrino anomaly. Likewise, one can investigate how robust is the determination of solar oscillation parameters, taking into account the presence of NSI.

We now turn to the robustness of solar oscillations parameter determination taking into account uncertainties in solar physics. One possibility is to consider random solar matter density [84]. It has been argued that a resonance between helioseismic and Alfvén waves might provide a physical mechanism for generating these fluctuations [85]. They can have an important effect upon neutrino conversion in matter [86, 87], as shown in Figs. 9. and 10. From the latter one sees that the determination of neutrino oscilla-

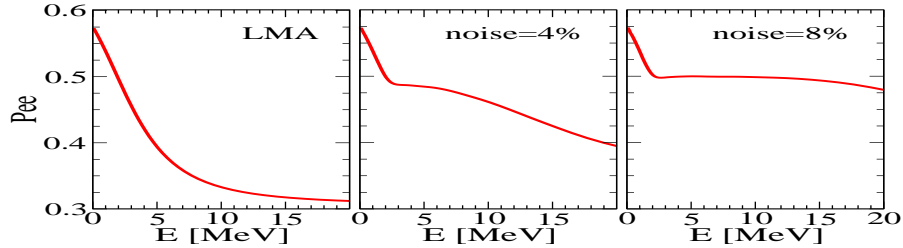


FIGURE 9. Effect of random matter density perturbations on the LMA-MSW solution. The left panel is for quiet Sun, middle and right panels correspond to $\xi = 4\%$ and $\xi = 8\%$, respectively, from [88]

tion parameters from a combined fit of KamLAND and solar data depends strongly on the magnitude of solar density fluctuations. Given the current neutrino oscilla-

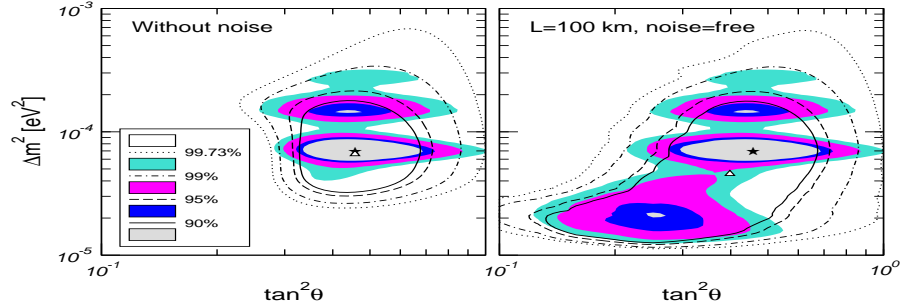


FIGURE 10. Allowed regions of neutrino oscillation parameters for the quiet Sun (left panel) and for a noisy Sun on a $L_0 = 100$ km spatial scale with arbitrary density noise magnitude ξ [88]. The lines and shaded regions correspond to the analyses of solar and solar+KamLAND data respectively.

rameters, the results of KamLAND imply new information on fluctuations in the solar environment on scales to which standard helioseismic tests are largely insensitive. The sensitivity of present solar neutrino + KamLAND data to the solar noise parameter ξ as a function of the correlation length L_0 , when neutrino oscillation parameters are varied inside the present LMA region has been given in [88].

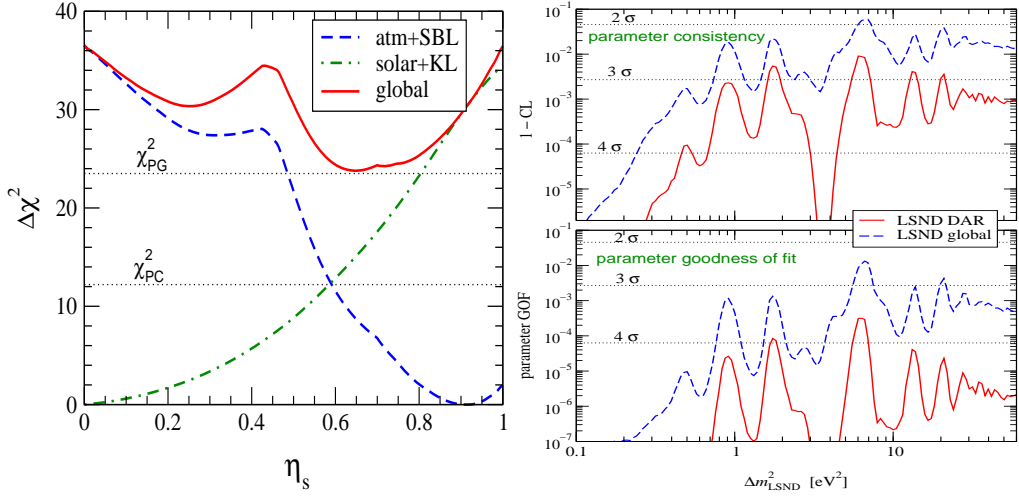


FIGURE 11. $\Delta\chi^2_{\text{SOL}}$, $\Delta\chi^2_{\text{ATM+SBL+KAMLAND}}$ and $\bar{\chi}^2_{\text{global}}$ as a function of η_s in (2+2) oscillation schemes (left). The right panel show how (3+1) schemes are still acceptable at 3σ . From Ref. [45]

LSND

The LSND experiment [43], which sees evidence for $\bar{\nu}_e$ appearance in a $\bar{\nu}_\mu$ beam, is suggestive of oscillations on a scale much higher than those indicated by solar and atmospheric data. All other experiments such as the short baseline disappearance experiments Bugey [89] and CDHS [90], as well as the KARMEN neutrino experiment [91] report no evidence for oscillations.

Prompted by recent improved solar and atmospheric data, ref. [45] has re-analysed the four-neutrino description of all current neutrino oscillation data, including the LSND evidence. The higher degree of rejection for non-active solar and atmospheric oscillation solutions implied by the SNO neutral current result, and by the latest 1489-day Super-K atmospheric neutrino data, allows one to rule out (2+2) oscillation schemes proposed to reconcile LSND with the rest of current oscillation data. Using an improved goodness of fit (gof) method especially sensitive to the combination of data sets one obtains a gof of only 1.6×10^{-6} for (2+2) schemes. This is illustrated by the left panel in Fig. 11. Also shown in the left panel of Fig. 11 are the values χ^2_{PC} and χ^2_{PG} relevant for parameter consistency and parameter g.o.f., respectively. The right panel displays the compatibility of LSND with solar+atmospheric+NEV data in (3+1) schemes. In the upper panel we show the C.L. of the parameter consistency whereas in the lower panel we show the parameter g.o.f. for fixed values of Δm^2_{LSND} . The analysis is performed both for the global [43] and for the DAR [92] LSND data samples.

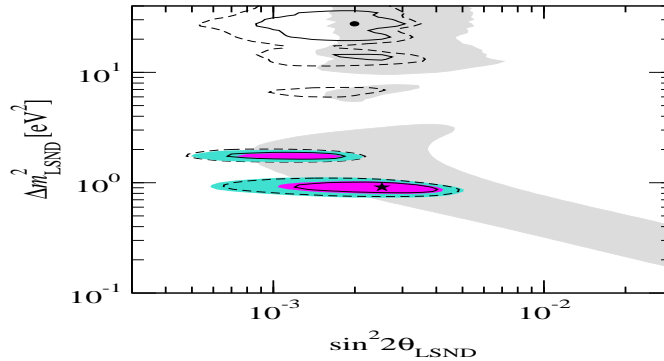


FIGURE 12. Allowed regions at 90 and 99 % C.L. for 3+1 schemes with (colored) and without (solid and dashed lines) information coming from cosmology. The grey region is the 99% C.L. LSND region [95]

In summary one finds that the strong preference of oscillations into active neutrinos implied by solar+KamLAND, as well as atmospheric neutrino data, rules out (2+2) mass schemes, whereas (3+1) schemes are strongly disfavoured, but not ruled out, by short-baseline experiments.

There are, in addition, recent data from cosmology, including CMB data from WMAP [46] and data from 2dFGRS large scale structure surveys [93] that can be used to further constrain 4-neutrino schemes [48, 94]. The result of such analysis, based on the data of [49] is illustrated in Fig. 12. Thus one sees that cosmology cuts the large Δm_{LSND}^2 values. In summary, one finds that even (3+1) schemes are strongly disfavoured by current data, bringing the LSND hint to a more puzzling status that led people to suggest solutions as radical as the violation of CPT [12].

THREE-NEUTRINO PARAMETERS

Given the stringent bounds on four-neutrino schemes derived from current global fits it is relevant to analyse in more detail the constraints on three-neutrino parameters, in particular on θ_{13} , so far neglected. This has been done in detail in Ref. [76]. Here we summarize the update to be presented in [96] including the most recent data, such as the K2K data which has recently observed positive indications of neutrino oscillation in a 250 km long-baseline setup [97]. The projections of the five-dimensional parameter space are displayed in Fig. 13. The goodness of the determination of the five 3-neutrino oscillation parameters is illustrated in Fig. 14. Both hierarchical and quasi-degenerate neutrino mass spectra, illustrated in Fig. 15, are compatible with current data.

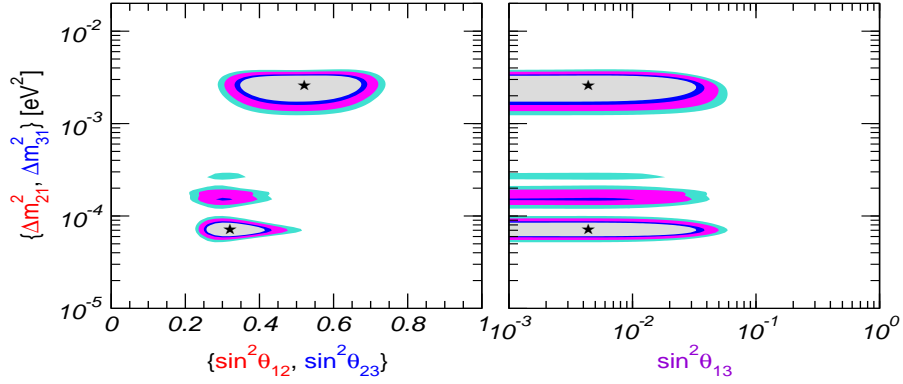


FIGURE 13. 90, 95, 99% C.L. and 3σ regions of solar and atmospheric oscillation parameters versus the corresponding mixing parameters (left) and versus $\sin^2 \theta_{13}$ from [96]

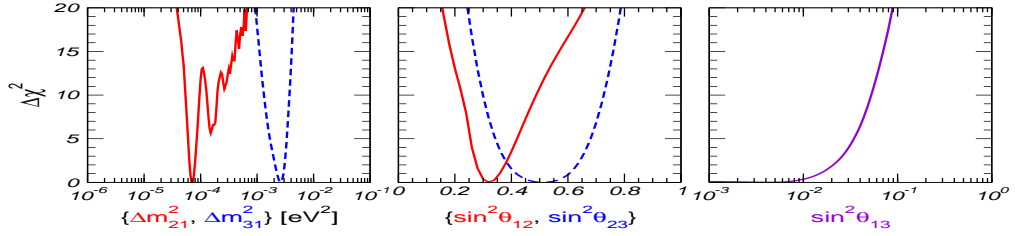


FIGURE 14. Determining the five 3-neutrino oscillation parameters, from [96]

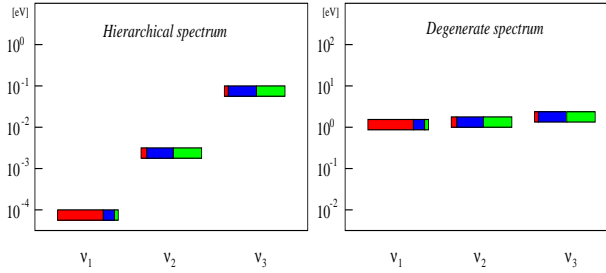


FIGURE 15. Hierarchical (left) and quasi-degenerate neutrino spectra (right).

Neutrino factories and the angle θ_{13}

Neutrino factories aim at probing the lepton mixing angle θ_{13} with much better sensitivity than possible at present, and thus open the door to the possibility of leptonic CP violation [53, 54]. We have already discussed both the hierarchical nature of neutrino mass splittings indicated by the observed solar and atmospheric neutrino anomalies, as well as the stringent bound on θ_{13} that follows from reactor experiments Chooz and Palo Verde. We also mentioned that the leptonic CP violation associated to the

standard Dirac phase present in the simplest three-neutrino system disappears as two neutrinos become degenerate and/or as $\theta_{13} \rightarrow 0$ [52]. As a result, although the large mixing associated to LMA-MSW certainly helps, direct leptonic CP violation tests in oscillation experiments will be a very demanding task for neutrino factories.

Refs. [98, 99] considered the impact of non-standard interactions of neutrinos on the determination of neutrino mixing parameters at a neutrino factory using $\bar{\nu}_e \rightarrow \bar{\nu}_\mu$ “golden channels” for the measurement of θ_{13} . One finds that even a small residual NSI leads to a drastic loss in sensitivity in θ_{13} , of up to two orders of magnitude ⁶.

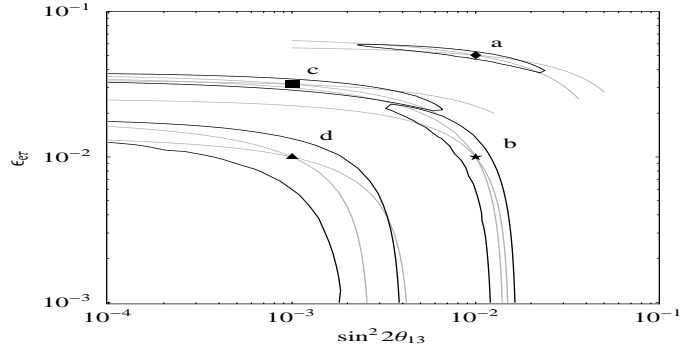


FIGURE 16. 99% C.L. allowed regions (black lines) in $\sin^2 2\theta_{13}-\epsilon_{e\tau}$ for different input values indicated by the points, at a baseline of 3000 km, from [98]. Lines of constant event rates are displayed in grey.

Therefore the design of a neutrino factory should include a near-site detector capable of monitoring the possible presence of non-standard interactions. For more details on the confusion between NSI and oscillations in the e-tau channel see [99].

ABSOLUTE NEUTRINO MASS SCALE

Oscillations are sensitive only to neutrino mass splittings and mixing angles, not to the absolute scale of neutrino mass. Tritium end-point [38] and $\beta\beta_{0\nu}$ experiments [100, 101] may determine the absolute scale of neutrino mass [102].

In contrast to the 2-neutrino mode, neutrinoless double beta decay [101, 103] violates L by 2 units. It is expected to occur due to the exchange of massive neutrinos (mass mechanism), provided they are Majorana particles. The phase space advantage of $\beta\beta_{0\nu}$ opens some hope of overcoming the suppression due to the L-violating Majorana neutrino propagator [8]. Now that neutrino masses have been established, one

⁶ This can be somewhat overcome if two baselines are combined.

expects a non-vanishing $\beta\beta_{0\nu}$ decay rate. The amplitude is proportional to the parameter $\langle m_\nu \rangle = \sum_j K_{ej}^2 m_j$ which can be given as,

$$\langle m_\nu \rangle = c_{12}^2 c_{13}^2 m_1 + s_{12}^2 c_{13}^2 e^{i\alpha} m_2 + s_{13}^2 e^{i\beta} m_3$$

in terms of three masses m_i , two angles θ_{12} and θ_{13} , and two CP violating phases: α, β . Using current neutrino oscillation data one can display the attainable $\langle m_\nu \rangle$ values for a normal (left) versus an inverse hierarchy (right), as shown in Fig. 17. Different shades (colors) correspond to different CP sign combinations among the three neutrinos. One

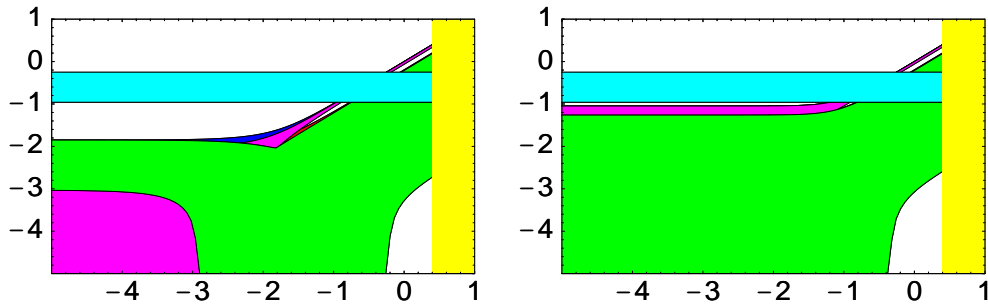


FIGURE 17. $\text{Log } \langle m_\nu \rangle / \text{eV}$ versus $\text{Log } m_1 / \text{eV}$, $\beta\beta_{0\nu}$ (horizontal band) and tritium sensitivities (vertical)

sees from Fig. 17 that $\beta\beta_{0\nu}$ is too small if the neutrinos obey a normal mass hierarchy ($\langle m_\nu \rangle \lesssim 0.01$ eV at left part of left panel). In contrast, it is enhanced by about an order of magnitude if the hierarchy is inverted ($\langle m_\nu \rangle \lesssim 0.1$ eV at left part of right panel), or in the quasi-degenerate limit ($\langle m_\nu \rangle \sim 1$ eV right parts of either panel in Fig. 17). Progress in this field will come about through the improvement of the current upper limit for $\langle m_\nu \rangle \leq 0.3$ eV in a new generation of $\beta\beta_{0\nu}$ experiments, such as GENIUS [100, 101], an improvement in the accuracy of nuclear matrix elements (currently a with factor ~ 2) [103, 104], as well as an improvement in the current upper limit from tritium experiments: $m_1 \leq 2.5$ eV in experiments such as KATRIN [105].

The importance of $\beta\beta_{0\nu}$ in deciding the nature of neutrinos goes far beyond the details of the mass mechanism. The connection between the two is given by the “black-box theorem” which states what, in a gauge theory, whatever the mechanism for inducing $\beta\beta_{0\nu}$ is, it is bound to also yield a Majorana neutrino mass at some level, and vice-versa, as illustrated by fig. 18 [106].

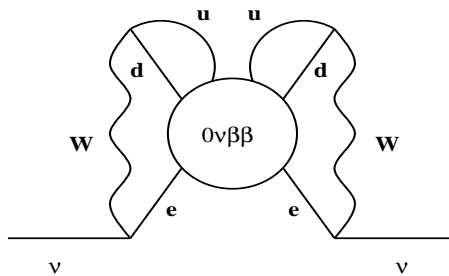


FIGURE 18. The black-box $\beta\beta_{0\nu}$ argument, from [106].

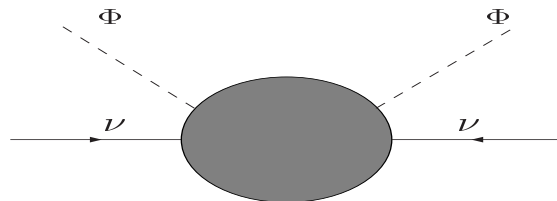


FIGURE 19. Dimension 5 operator for neutrino mass.

NEUTRINO THEORIES

The simplest way to generate neutrino masses is via the dimension–five operator of Fig. 19 [18]. Such may arise from gravity itself, though in this case the masses generated are much smaller than indicated by current solar and atmospheric experiments. Thus one needs to appeal to physics at a lower scale. The seesaw with a scale in the unification range can do the job [107]. An extreme view of this approach is the idea of neutrino unification, advocated in [23]⁷ and [24], and illustrated in Fig. 20. In this picture, neutrino masses behave like the gauge coupling constants of the Standard Model [108], which

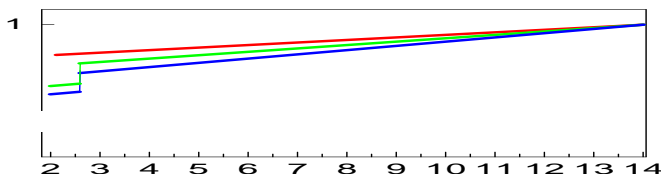


FIGURE 20. Neutrino mass in eV versus $\text{Log } M_X/\text{GeV}$, where M_X is the neutrino unification scale

⁷ Only the CP conserving variant of the model in [23] is ruled out by current solar data.

merge at high energies as they are evolved via the renormalization group, due to the presence of supersymmetry [109, 110, 111]. Such a simple theoretical ansatz provides the most natural framework for having a neutrino mass scale potentially observable in tritium and $\beta\beta_{0\nu}$ experiments, as well as cosmology, leading to the so-called quasi-degenerate neutrino spectrum (right panel of Fig. 15).

In the variant of this idea proposed in [24] the discrete non-Abelian symmetry A_4 , valid at some high-energy scale, is responsible for the degenerate neutrino masses, without spoiling the hierarchy of charged-lepton masses. Mass splittings and mixing angles are induced radiatively in the context of softly broken supersymmetry. The model predicts that the atmospheric angle is necessarily maximal and that either the mixing parameter θ_{13} is zero or pure imaginary, leading to maximal CP violation in neutrino oscillations [112]. The solar angle is unpredicted, but can be large. The quark mixing matrix is also calculable in a similar way. Large lepton mixing angles are compatible with the smallness of the quark mixing angles because only neutrinos are degenerate. Neutrinoless double beta decay and flavor violating tau decays such as $\tau \rightarrow \mu\gamma$ should be in the experimentally accessible range.

Low energy supersymmetry as the origin of neutrino mass [25, 26, 27] provides a viable alternative to the seesaw. In this case Weinberg's operator arises from weak-scale physics [25, 26, 27] in theories with spontaneous breaking of R parity [28, 29, 30]. These lead effectively to bilinear violation [31]. Neutrino mixing angles can be probed at accelerator experiments, which have therefore the potential to falsify the model. Alternative low energy mechanisms for neutrino mass generation are the models of Babu [36] and Zee [37] and variants thereof.

All in all, there is no clear "road map" for the ultimate theory of neutrinos, since we can not predict neutrino properties from first principles: we do not know the underlying scale nor the mechanism involved. Last, but not least, we lack a fundamental theory of flavour. The neutrino mass tale is far from told, despite the extraordinary revolution brought about by the experimental discovery of neutrino mass.

ACKNOWLEDGMENTS

I am thankful to Joe Schechter for his insights and friendship. This work was supported by a Humboldt Research Award (J. C. Mutis Prize), by Spanish grant BFM2002-00345,

by the European Commission RTN grant HPRN-CT-2000-00148 and the European Science Foundation Neutrino Astrophysics Network. I thank Martin Hirsch for discussions on double beta decay, M Maltoni and M A Tórtola for advancing results of [96]

REFERENCES

1. Fukuda, Y., et al., *Phys. Rev. Lett.*, **81**, 1562–1567 (1998).
2. Fukuda, S., et al., *Phys. Lett.*, **B539**, 179–187 (2002).
3. Ahmad, Q. R., et al., *Phys. Rev. Lett.*, **89**, 011301 (2002).
4. Ahmad, Q. R., et al., *Phys. Rev. Lett.*, **89**, 011302 (2002).
5. Eguchi, K., et al., *Phys. Rev. Lett.*, **90**, 021802 (2003).
6. Schechter, J., and Valle, J. W. F., *Phys. Rev.*, **D22**, 2227 (1980).
7. Cheng, T. P., and Li, L.-F., *Phys. Rev.*, **D22**, 2860 (1980).
8. Schechter, J., and Valle, J. W. F., *Phys. Rev.*, **D24**, 1883 (1981), err. *Phys. Rev. D*25, 283 (1982).
9. Mohapatra, R. N., and Senjanovic, G., *Phys. Rev.*, **D23**, 165 (1981).
10. Mikheev, S. P., and Smirnov, A. Y., *Sov. J. Nucl. Phys.*, **42**, 913–917 (1985).
11. Wolfenstein, L., *Phys. Rev.*, **D17**, 2369 (1978).
12. Pakvasa, S., and Valle, J. W. F. (2003), prepared for Special Issue of Proceedings of the Indian National Academy of Sciences on Neutrinos, hep-ph/0301061, and references therein.
13. Gonzalez-Garcia, M. C., and Nir, Y. (2002); Altarelli, G. and Feruglio, F. hep-ph/0306265.
14. Bilenky, S. M., Giunti, C., and Grimus, W., *Eur. Phys. J.*, **C1**, 247–253 (1998).
15. Gell-Mann, M., Ramond, P., and Slansky, R. (1979), print-80-0576 (CERN).
16. Yanagida, T. (1979), ed. Sawada and Sugamoto (KEK, 1979).
17. Reines, F., Sobel, H. W., and Pasierb, E., *Phys. Rev. Lett.*, **45**, 1307 (1980).
18. Weinberg, S. (1980), harvard Univ. Cambridge - HUTP-80-A038 (80,REC.DEC) 16p.
19. Chikashige, Y., Mohapatra, R. N., and Peccei, R. D., *Phys. Lett.*, **B98**, 265 (1981).
20. Schechter, J., and Valle, J. W. F., *Phys. Rev.*, **D25**, 774 (1982).
21. Kuzmin, V. A., Rubakov, V. A., and Shaposhnikov, M. E., *Phys. Lett.*, **B155**, 36 (1985).
22. Fukugita, M., and Yanagida, T., *Phys. Lett.*, **B174**, 45 (1986).
23. Chankowski, P., Ioannian, A., Pokorski, S., and Valle, J. W. F., *Phys. Rev. Lett.*, **86**, 3488 (2001).
24. Babu, K. S., Ma, E., and Valle, J. W. F., *Phys. Lett.*, **B552**, 207–213 (2003).
25. Diaz, M. A., et. al. (2003), hep-ph/0302021 *Phys. Rev. D* in press.
26. Hirsch, M., et. al., *Phys. Rev.*, **D62**, 113008 (2000), err-ibid.D65:119901,2002.
27. Romao, J. C., et. al., *Phys. Rev.*, **D61**, 071703 (2000).
28. Ross, G. G., and Valle, J. W. F., *Phys. Lett.*, **B151**, 375 (1985).
29. Ellis, J. R., Gelmini, G., Jarlskog, C., Ross, G. G., and Valle, J. W. F., *Phys. Lett.*, **B150**, 142 (1985).
30. Masiero, A., and Valle, J. W. F., *Phys. Lett.*, **B251**, 273–278 (1990).
31. Diaz, M. A., Romao, J. C., and Valle, J. W. F., *Nucl. Phys.*, **B524**, 23–40 (1998).
32. Hirsch, M., Porod, W., Romao, J. C., and Valle, J. W. F., *Phys. Rev.*, **D66**, 095006 (2002).
33. Porod, W., Hirsch, M., Romao, J., and Valle, J. W. F., *Phys. Rev.*, **D63**, 115004 (2001).

34. Restrepo, D., Porod, W., and Valle, J. W. F., *Phys. Rev.*, **D64**, 055011 (2001).
35. Ma, E. *Mod. Phys. Lett.*, **17**, 1259 (2002); Aristizabal, D. et. al., hep-ph/0304141, *Phys. Rev. D*.
36. Babu, K. S., *Phys. Lett.*, **B203**, 132 (1988).
37. Zee, A., *Phys. Lett.*, **B93**, 389 (1980).
38. Hagiwara, K., et al., *Phys. Rev.*, **D66**, 010001 (2002).
39. Peltoniemi, J. T., and Valle, J. W. F., *Nucl. Phys.*, **B406**, 409–422 (1993).
40. Peltoniemi, J. T., Tommasini, D., and Valle, J. W. F., *Phys. Lett.*, **B298**, 383–390 (1993).
41. Caldwell, D. O., and Mohapatra, R. N., *Phys. Rev.*, **D48**, 3259–3263 (1993).
42. Giunti, C., and Laveder, M. (2000), <http://www.to.infn.it/~giunti/NU/>.
43. Aguilar, A., et al., *Phys. Rev.*, **D64**, 112007 (2001).
44. Maltoni, M., Schwetz, T., Tortola, M. A., and Valle, J. W. F., *Phys. Rev.*, **D67**, 013011 (2003).
45. Maltoni, M., Schwetz, T., Tortola, M. A., and Valle, J. W. F., *Nucl. Phys.*, **B643**, 321–338 (2002).
46. Spergel, D. N., et al. (2003), astro-ph/0302209.
47. Crotty, P., Lesgourgues, J., and Pastor, S., *Phys. Rev.*, **D67**, 123005 (2003).
48. Elgaroy, O., and Lahav, O., *JCAP*, **0304**, 004 (2003).
49. Hannestad, S. (2003), astro-ph/0303076.
50. Tegmark, M., Hamilton, A. J. S., and Xu, Y., *Mon. Not. Roy. Astron. Soc.*, **335**, 887–908 (2002).
51. Apollonio, M., et al., *Phys. Lett.*, **B466**, 415–430 (1999).
52. Schechter, J., and Valle, J. W. F., *Phys. Rev.*, **D21**, 309 (1980).
53. Apollonio, M., et al. (2002), hep-ph/0210192.
54. Freund, M., Huber, P., and Lindner, M., *Nucl. Phys.*, **B615**, 331–357 (2001).
55. Albright, C., et al. (2000), hep-ex/0008064.
56. Cervera, A., et al., *Nucl. Phys.*, **B579**, 17–55 (2000).
57. Schechter, J., and Valle, J. W. F., *Phys. Rev.*, **D23**, 1666 (1981).
58. Kayser, B., *Phys. Rev.*, **D26**, 1662 (1982).
59. Nieves, J. F., *Phys. Rev.*, **D26**, 3152 (1982).
60. Pal, P. B., and Wolfenstein, L., *Phys. Rev.*, **D25**, 766 (1982).
61. Doi, M., Kotani, T., Nishiura, H., Okuda, K., and Takasugi, E., *Phys. Lett.*, **B102**, 323 (1981).
62. Wolfenstein, L., *Phys. Lett.*, **B107**, 77 (1981).
63. Barger, V., Glashow, S. L., Langacker, P., and Marfatia, D., *Phys. Lett.*, **B540**, 247–251 (2002).
64. Barranco, J., et. al., *Phys. Rev.*, **D66**, 093009 (2002);
Akhmedov, E., Pulido, J., *Phys. Lett.*, **B553**, 7 (2003).
65. Guzzo, M., et al., *Nucl. Phys.*, **B629**, 479–490 (2002);
Davidson, S., Pena-Garay, C., Rius, N., and Santamaria, A., *JHEP*, **03**, 011 (2003).
66. Fukuda, Y., et al., *Phys. Rev. Lett.*, **82**, 2644–2648 (1999).
67. Fukuda, Y., et al., *Phys. Lett.*, **B433**, 9–18 (1998).
68. Fukuda, Y., et al., *Phys. Lett.*, **B436**, 33–41 (1998).
69. Fukuda, Y., et al., *Phys. Lett.*, **B467**, 185–193 (1999).
70. Shiozawa, M. (2002), talk at Neutrino 2002, <http://neutrino2002.ph.tum.de/>.
71. Surdo, A., *Nucl. Phys. Proc. Suppl.*, **110**, 342–345 (2002).
72. Cleveland, B. T., et al., *Astrophys. J.*, **496**, 505–526 (1998).
73. Abdurashitov, J. N., et al., *Phys. Rev. Lett.*, **83**, 4686 (1999).

74. Altmann, M., et al., *Phys. Lett.*, **B490**, 16–26 (2000).
75. Maltoni, M., Schwetz, T., and Valle, J. W. F., *Phys. Rev.*, **D65**, 093004 (2002).
76. Gonzalez-Garcia, M., Maltoni, M., Pena-Garay, C., Valle, J. W., *Phys. Rev.*, **D63**, 033005 (2001).
77. Maltoni, M., Schwetz, T., and Valle, J. W. F., *Phys. Rev.*, **D67**, 093003 (2003).
78. Hall, L. J., Kostelecky, V. A., and Raby, S., *Nucl. Phys.*, **B267**, 415 (1986).
79. Valle, J. W. F., *Phys. Lett.*, **B199**, 432 (1987).
80. Guzzo, M. M., Masiero, A., and Petcov, S. T., *Phys. Lett.*, **B260**, 154–160 (1991).
81. Nunokawa, H., Qian, Y. Z., Rossi, A., and Valle, J. W. F., *Phys. Rev.*, **D54**, 4356–4363 (1996).
82. Fornengo, N., Maltoni, M., Bayo, R. T., and Valle, J. W. F., *Phys. Rev.*, **D65**, 013010 (2002).
83. Huber, P., and Valle, J. W. F., *Phys. Lett.*, **B523**, 151–160 (2001).
84. Balantekin, A. B., Fetter, J. M., and Loreti, F. N., *Phys. Rev.*, **D54**, 3941–3951 (1996).
85. Burgess, C. P., et al. (2003), astro-ph/0304462.
86. Nunokawa, H., Rossi, A., Semikoz, V. B., and Valle, J. W. F., *Nucl. Phys.*, **B472**, 495–517 (1996).
87. Bamert, P., Burgess, C. P., and Michaud, D., *Nucl. Phys.*, **B513**, 319–342 (1998).
88. Burgess, C., et al., *Astrophys. J.*, **588**, L65 (2003). See also Guzzo, M., et al., hep-ph/0303203
89. Declais, Y., et al., *Nucl. Phys.*, **B434**, 503–534 (1995).
90. Dydak, F., et al., *Phys. Lett.*, **B134**, 281 (1984).
91. Armbruster, B., et al., *Phys. Rev.*, **D65**, 112001 (2002).
92. Church, E. D., Eitel, K., Mills, G. B., and Steidl, M., *Phys. Rev.*, **D66**, 013001 (2002).
93. Peacock, J. A., et al., *Nature*, **410**, 169–173 (2001).
94. Elgaroy, O., et al., *Phys. Rev. Lett.*, **89**, 061301 (2002).
95. Maltoni, M., Schwetz, T., Tortola, M. A., and Valle, J. W. F. (2003), hep-ph/0305312.
96. Maltoni, M., Schwetz, T., Tortola, M. A., and Valle, J. W. F. (2003), in preparation.
97. Ahn, M. H., et al., *Phys. Rev. Lett.*, **90**, 041801 (2003).
98. Huber, P., Schwetz, T., and Valle, J. W. F., *Phys. Rev. Lett.*, **88**, 101804 (2002).
99. Huber, P., Schwetz, T., and Valle, J. W. F., *Phys. Rev.*, **D66**, 013006 (2002).
100. Klapdor-Kleingrothaus, H. V., et al. (1999), hep-ph/9910205.
101. Morales, A., *Nucl. Phys. Proc. Suppl.*, **77**, 335–345 (1999).
102. Klapdor-Kleingrothaus, H. V., Hirsch, M., *Z. Phys.*, **A359**, 361 (1997); Minakata, H. and Yasuda, O., *Phys. Rev.* **D56**, 1692 (1997); Klapdor-Kleingrothaus, H. V., Pas, H., and Smirnov, A. Y., *Phys. Rev.*, **D63**, 073005 (2001); Feruglio, F. Strumia, A. and Vissani, F., *Nucl. Phys.* **B637**, 345 (2002)
103. Faessler, A., and Simkovic, F., *Prog. Part. Nucl. Phys.*, **46**, 233–251 (2001).
104. Elliott, S. R., and Vogel, P., *Ann. Rev. Nucl. Part. Sci.*, **52**, 115–151 (2002).
105. Osipowicz, A., et al. (2001), hep-ex/0109033.
106. Schechter, J., and Valle, J. W. F., *Phys. Rev.*, **D25**, 2951 (1982).
107. Black, D., et al. *Phys. Rev.*, **62**, 073015 (2000); Ross, G., and Velasco-Sevilla, L., *Nucl. Phys.*, **B653**, 3 (2003); King, S. hep-ph/0208270; Grimus, W., hep-ph/0307149
108. Langacker, P., and Polonsky, N., *Phys. Rev.*, **D52**, 3081–3086 (1995).
109. Casas, J. A., Espinosa, J. R., Ibarra, A., and Navarro, I., *Nucl. Phys.*, **B569**, 82–106 (2000).
110. Frigerio, M., and Smirnov, A. Y., *JHEP*, **02**, 004 (2003).
111. Antusch, S., Kersten, J., Lindner, M., and Ratz, M., *Phys. Lett.*, **B538**, 87–95 (2002).
112. Grimus, W., and Lavoura, L., hep-ph/0305309